J Mol Model (2013) 19:1553–1563
DOI 10.1007/s00894-012-1723-6

ORIGINAL PAPER

Comparative study on electronic structures and optical properties of indoline and triphenylamine dye sensitizers for solar cells

Cai-Rong Zhang · Li Liu · Jian-Wu Zhe · Neng-Zhi Jin · Li-Hua Yuan · Yu-Hong Chen · Zhi-Qiang Wei · You-Zhi Wu · Zi-Jiang Liu · Hong-Shan Chen

Received: 3 November 2012 / Accepted: 3 December 2012 / Published online: 28 December 2012

Abstract The computations of the geometries, electronic structures, dipole moments and polarizabilities for indoline and triphenylamine (TPA) based dye sensitizers, including D102, D131, D149, D205, TPAR1, TPAR2, TPAR4, and TPAR5, were performed using density functional theory, and the electronic absorption properties were investigated *via* time-dependent density functional theory with polarizable continuum model for solvent effects. The population analysis indicates that the donating electron capability of TPA is better than that of indoline group. The reduction driving forces for the oxidized D131 and TPAR1 are slightly larger than that of other dyes because of their lower highest occupied molecular orbital level. The absorption properties and molecular orbital analysis suggest that the TPA and 4-(2,2diphenylethenyl)phenyl substituent indoline groups are effective chromophores in intramolecular charge transfer (IMCT), and they play an important role in sensitization of dye-sensitized solar cells (DSCs). The better performance of D205 in DSCs results from more IMCT excited states with larger oscillator strength and higher light harvesting efficiency. While for TPA dyes, the longer conjugate bridges generate the larger oscillator strength and light harvesting efficiency, and the TPAR1 and TPAR4 have larger free energy change for electron injection and dye regeneration.

Keywords Absorption spectra · Density functional theory · Dye sensitized solar cells · Electronic structure · Organic dye sensitizer

C.-R. Zhang · L. Liu · L.-H. Yuan · Y.-H. Chen · Z.-Q. Wei
Department of Applied Physics, Lanzhou University of Technology, Lanzhou, Gansu 730050, China

C.-R. Zhang (✉) · Y.-H. Chen · Z.-Q. Wei · Y.-Z. Wu
State Key Laboratory of Gansu Advanced Non-ferrous Metal Materials, Lanzhou University of Technology, Lanzhou, Gansu 730050, China
e-mail: zhcrxy@lut.cn

J.-W. Zhe · N.-Z. Jin
Gansu Computing Center, Lanzhou, Gansu 730030, China

Z.-J. Liu
Institute of Electronic Information Science and Technology, Lanzhou City University, Lanzhou, Gansu 730070, China

H.-S. Chen
College of Physics and Electronic Engineering, Northwest Normal University, Lanzhou, Gansu 730070, China

Introduction

The dye-sensitized solar cells (DSC) have attracted much attention because of easy fabrication, lower cost, and relatively higher efficiency [1–5]. The main components of DSC are dye sensitizers, anode, cathode, and electrolyte. All of them can affect the performance of DSC. Especially, the dye sensitizers, which take the function of light harvesting and photo-excited electron injection in DSC, have a significant influence on the photon-to-current conversion efficiency (PCE) [6–11]. Up to now, the dye sensitizers, which were designed, synthesized and characterized in order to improve the PCE of DSC, can be classified into metal-organic complexes and metal-free organic dyes [7–10]. In metal-organic complexes, the noble metal ruthenium polypyridyl complexes, including N3 dye *cis*-[Ru-(4,4′-COOH-2,2′-bpy)$_2$(NCS)$_2$] and "black dye" (tri(cyanato)-2,2′,2″-terpyridyl-4,4′,4″-tricarboxylate)Ru(II)), were proved to be the best dye sensitizers with overall energy conversion efficiency greater than 10 % under air mass (AM) 1.5 irradiation [12–14]. On the other hand, metal-free organic dyes sensitizers, such as cyanines [15–17], hemicyanines [18, 19], triphenylmethanes [8, 20, 21], perylenes [22–26], coumarins

[27–29], porphyrins [30–35], squaraines [36–38], indoline [39, 40], and azulene-based dyes [41] *etc.*, were also developed due to their high molar absorption coefficient, relatively simple synthetic procedure, various structures and lower cost. Recently, the 12.3 % PCE has been achieved by cosensitization of donor-π-bridge-acceptor zinc porphyrin dye YD2-*o*-C8 with another triphenylamine-based organic dye Y123 [42]. So the development of novel organic dye sensitizer is still a promising method to improve the PCE of DSC.

Indoline dyes had been recognized as better dye sensitizer since indoline sensitized DSCs were reported [43–46]. The PCE of 9.03 % was achieved by the optimized thickness of indoline dye D149-sensitized DSC for ionic-liquid-based electrolytes [47]. It was also found that indoline dyes D102, D131, and D149 can be utilized to fabricate solid-state DSCs [48, 49]. Using the stable organic radical 2,2,6,6-Tetramethyl-1-piperidinyloxy as redox system, the DSC based on D149 yielded PCE of 5.4 % [50]. Under AM1.5 irradiation, the 7.2 % PCE for DSC based on ionic liquids and organic dye sensitizer D205 was reported [40], and D205 gave higher PCE 9.52 % of organic DSCs using an anti-aggregation reagent chenodeoxycholic acid [51]. Based upon calculating the lowest unoccupied molecular orbital (LUMO) of three indoline dyes (D131, D102, and D149) and comparing the PCE of DSCs fabricated using those dyes, it was found that the efficiencies of charge injection was determined by the extent to which the LUMO of the dye falls on its anchoring group acetic acid [52]. To understand the structures and properties of dyes, as well as for the sensitized mechanism of DSCs, the theoretical investigations of the light absorption and fluorescence properties of indoline dyes D102, D131, and D149 were reported [53].

Triphenylamine (TPA) dyes are also a promising sensitizer family for DSCs [8, 20, 54–56]. The synthesis and photophysical/electrochemical properties of TPA-based dyes TPAR1, TPAR2, TPAR4, and TPAR5 as well as their applications in DSCs were reported, and the DSCs based on TPAR4 approached the 5.84 % PCE under AM1.5 irradiation [20]. The anchoring group in indoline dyes (D102, D131, D149, and D205) and TPA-based dyes (TPAR1, TPAR2, TPAR4, and TPAR5) are acetic acid (see Fig. 1). So, the adsorption behavior of dyes at the semiconductor surface should be similar. Moreover, most of these dyes contain rhodanine-3-acetic acid as electron acceptor. But, what are the differences in electronic structures of the dyes? What are the effective chromophores in the sensitization of DSCs? How does the different moiety modify the electronic structures and absorption properties? What are the reasons that induce better performance of D205 and TPAR4 in DSCs? To answer the above questions, the geometries, elelctronic structures, dipole moments, and polarizabilities, as well as absorption properties of indoline dyes D102, D131, D149, D205 and TPA-based dyes TPAR1, TPAR2, TPAR4, TPAR5 were calculated by using density functional theory (DFT) and time-dependent DFT (TDDFT). Based upon the calculated results, we analyzed the differences in electronic structures, the effective chromophores in the sensitization, and the role of different moieties in modifying the electronic structures and absorption properties. Also, we further investigated the reasons that induce different performance of dyes in DSCs.

Computational methods

The computations of the geometries, electronic structures, as well as polarizabilities for dye sensitizers were performed using DFT with the Gaussian 09 package [57]. The density functional was treated in terms of Becke's three parameters gradient-corrected exchange potential and the Lee-Yang-Parr gradient-corrected correlation potential (B3LYP) [58–61], and all calculations were performed without any symmetry constraints with the polarized split-valence 6–31G* basis sets. The electronic absorption spectra require the calculation of allowed excitations and oscillator strengths. The calculations were carried out using TDDFT method in gas phase and solvent. Usually, the electronic excitations of dye sensitizers with good performance in DSC are charge transfer (CT) processes. So, the different exchange-correlation functionals (B3LYP, PBE0 [62], and long-range-corrected hybrid functional CAM-B3LYP [63]) and basis sets (6–31G*, 6–31G(d, p), and 6–31+G(d,p)) were adopted for the calculations of electronic absorption spectra in order to obtain the appropriate description of CT excited states. The non-equilibrium version of the polarizable continuum model (PCM) [64] was adopted for considering the solvent effects.

Results and discussion

Geometrical structures

The optimized geometries of the dyes are shown in Fig. 1, and the hydrogen atoms in dye molecules were omitted for clarity. The geometrical parameters of indoline and TPA dyes are listed in Tables 1 and 2, respectively. It is found that the geometric parameters of the same group in different dyes are very similar because the geometries are mainly determined by the localized interaction of chemical bonds. For example, the N-C bond length between indole and phenyl are about 0.141 nm in indoline dyes, and the corresponding N-C bond lengths in TPA-based dyes are very similar (about 0.14 nm). Furthermore, substituting CH_2=CH- groups for hydrogen atoms in the TPA moieties, extending π bridges in TPA dyes by using methane units, and introducing different acceptor groups into indoline dyes

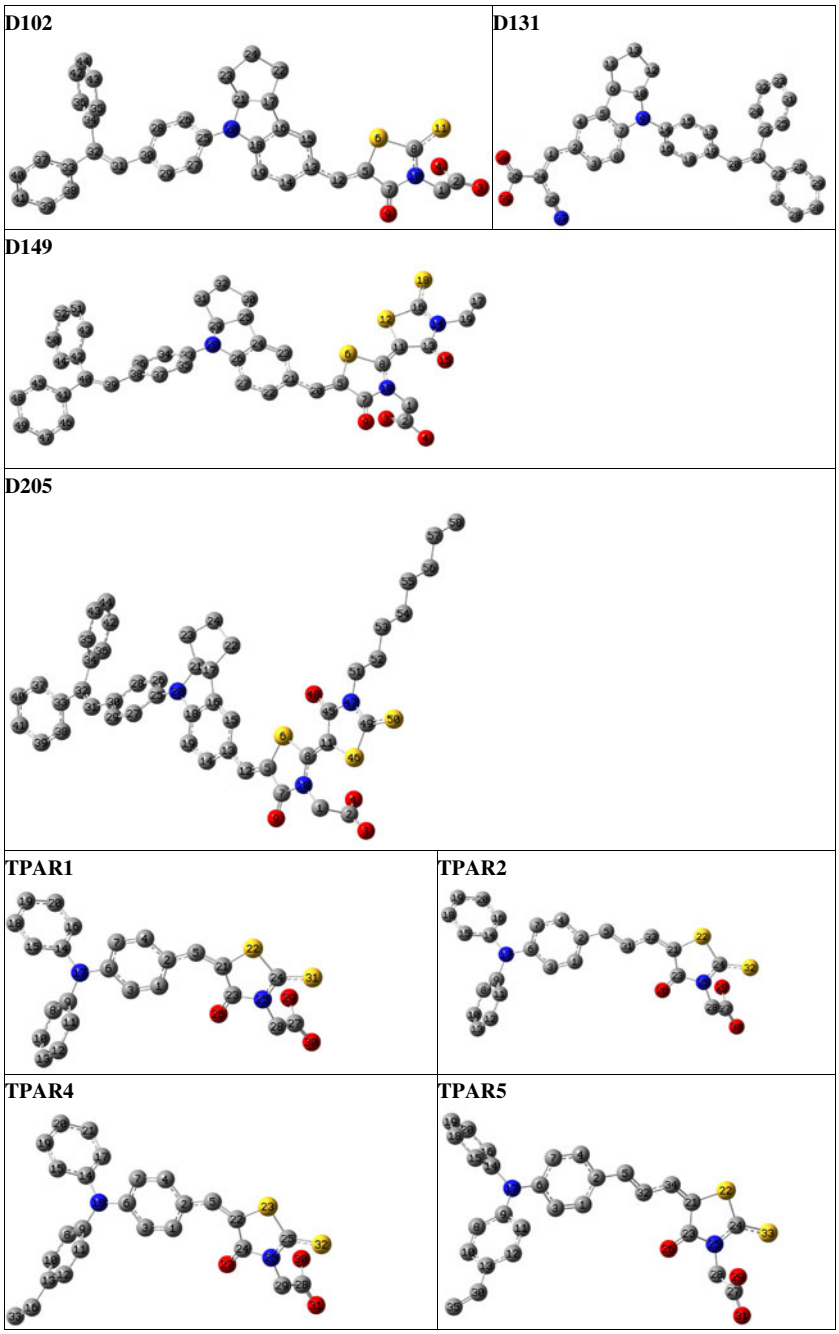

Fig. 1 The optimized geometrical structures of dye sensitizers. (B3LYP/6–31G*, H atoms are omitted for clarity, the gray colored spheres: C; the blue colored spheres: N; the red colored spheres: O; the yellow colored spheres: S)

slightly affect the local geometrical parameters. It is worthy to note that cyano acetic acid group (in D131) and rhodanine ring (in other dyes) are coplanar with benzene ring in indoline and TPA groups. This coplanar geometric character extends conjugate length, enhances electron delocalization, and the coplanarity between donor group and conjugate bridge is favorable for intramolecular charge transfer (IMCT) [65–70]. However, the rhodanine rings are not coplanar with acetic acid moieties. The breaking of coplanarity between the rhodanine rings and anchoring group acetic acid inhibits the recombination reactions at the interface of dyes and TiO_2 surface [71].

Electronic structures

In indoline dyes, arylamine moieties act as electron donor, and rhodanine-rings function as electron acceptor [48]. For TPA dyes, the TPA moieties and the rhodanine acetic acids take the role of the electron donor and the electron acceptor, respectively [20]. The carboxylic acids are anchor group that can attach to TiO_2 surface. The carbon-double-bond chains are conjugate bridges. The natural bond orbital (NBO) analysis was performed in order to analyze the electron populations of the dyes. The calculated natural charges that populated in the donor, conjugate bridge, and

Table 1 Selected bond lengths (in nm), bond angles (in degree), and dihedral angles (in degree) of the dyes D102, D131, D149 and D205

D102		D131		D149		D205	
1–2	0.152	34–36	0.149	1–2	0.152	2–1	0.153
1–10	0.145	1–34	0.137	1–10	0.146	1–10	0.145
5–12	0.136	34–35	0.143	5–20	0.136	5–12	0.136
12–13	0.144	1–2	0.144	20–21	0.144	12–13	0.144
20–25	0.141	9–14	0.141	28–33	0.141	20–25	0.141
30–31	0.147	19–20	0.147	38–39	0.147	30–31	0.147
31–32	0.136	20–21	0.136	39–40	0.136	31–32	0.136
2–1–10	115.1	36–34–1	117.0	2–1–10	110.6	2–1–10	116.1
5–12–13	132.3	34–1–2	132.7	5–20–21	132.2	5–12–13	132.2
20–25–26	121.0	9–14–16	120.5	28–33–34	121.0	20–25–26	121.1
30–31–32	130.5	19–20–21	130.6	38–39–40	130.6	30–31–32	130.9
7–10–1–2	99.5	2–1–34–36	179.9	7–10–1–2	82.5	7–10–1–2	99.4
5–12–13–14	179.7	34–1–2–4	179.3	5–20–21–22	177.7	5–12–13–14	179.5
18–20–25–27	51.4	7–9–14–16	51.5	26–28–33–35	51.0	18–20–25–27	51.5
30–31–32–33	173.5	19–20–21–22	173.3	38–39–40–41	173.6	30–31–32–3	173.7
8–11	0.165			8–11	0.138	8–11	0.137

the acceptor groups are listed in Table 3. The rhodanine-3-acetic acid and cyano acrylic acid groups are strong electronic withdrawing group. For indoline dyes, the natural charges of indoline groups are small, and the different terminal groups that connected with rhodanine-3-acetic acid slightly affect the charges of rhodanine-based acceptors. The charges populated in D131 acceptor moiety are more than that of other dyes. This indicates that cyano acrylic acid group has higher electron-withdrawing capability than that of rhodanine-3-acetic acid. However, for TPA-based dyes, the charges of acceptors in different dyes are very similar, and the charges of donors and conjugate bridges are more flexible. The conjugate bridges donate about 0.10 ~ 0.15 *e* to acceptor moieties. So, the conjugate bridges in the dyes have a double role, one is the linker between donor and acceptor, enhancing the electronic delocalization, and the other is a part of electron donor. Furthermore, for the dyes with rhodanine-based moieties, the natural charges of acceptor are very close (about −0.24 *e*). The difference between the dyes D102 and TPAR1 is the donor moieties. The charges of donor part in D102 (indoline group, 0.12 *e*) is slightly smaller than that in TPAR1 (TPA group, 0.14 *e*). This suggests that the donating electron capability of TPA is better than that of indoline.

The HOMO and LUMO energies, as well as the HOMO-LUMO gaps (E_g) of the dyes in gas phase and solvent are

Table 2 Selected bond lengths (in nm), bond angles (in degree), and dihedral angles (in degree) of the dyes TPAR1, TPAR2, TPAR4 and TPAR5

TPAR1		TPAR2		TPAR4		TPAR5	
27–28	0.152	27–28	0.152	28–29	0.152	27–28	0.152
25–28	0.145	25–28	0.145	26–29	0.145	25–28	0.145
5–21	0.137	21–33	0.137	5–22	0.137	21–34	0.137
5–2	0.145	5–2	0.145	5–2	0.145	5–2	0.145
6–17	0.140	6–17	0.141	6–18	0.140	6–17	0.141
17–14	0.143	17–14	0.143	14–18	0.143	17–14	0.143
27–28–25	115.1	27–28–25	115.1	28–29–26	115.1	27–28–25	115.1
2–5–21	135.6	31–32–21	126.7	2–5–22	135.6	32–34–21	126.7
6–17–14	120.8	6–17–14	120.7	6–18–14	120.6	6–17–14	120.4
23–25–28–27	97.9	23–25–28–27	98.3	6–18–9	121.1	23–25–28–27	99.9
1–2–5–21	0.4	4–2–5–31	179.2	1–2–5–22	1.2	4–2–5–32	178.9
3–6–17–9	28.8	3–6–17–9	31.4	3–6–18–9	30.1	3–6–17–9	32.6
		5–31–33–21	179.9	2–5–22–24	0.6	5–32–34–21	179.0
		31–33–21–22	179.8	13–16	0.147	13–30	0.147

Table 3 The calculated natural charges (*e*) of electron donor, conjugate bridge, and electron acceptor groups for the dyes

Dyes	Donor	Acceptor	Conjugate bridge
D102	0.124	−0.241	0.117
D131	0.159	−0.340	0.181
D149	0.125	−0.244	0.119
D205	0.119	−0.232	0.113
TPAR1	0.141	−0.238	0.097
TPAR2	0.089	−0.236	0.147
TPAR4	0.139	−0.236	0.097
TPAR5	0.086	−0.233	0.147

shown in Fig. 2. For indoline dyes, the substitution of rhodanine-3-acetic acid in D102 by cyano acrylic acid in D131 decrease HOMO about 0.09 eV, increase LUMO about 0.15 eV, and thus broaden E_g about 0.24 eV. However, the substitution of terminal S atom in D102 by another rhodanine-based moeties in D149 and D205 induce a slight up-shift for HOMO and down-shift for LUMO energies. Especially, compared with D149, the longer alkyl chain in D205 generates a tiny upper-shift of HOMO (about 0.02 eV) and LUMO (about 0.06 eV) because of the donor character of alkyl chain. As to TPA dyes, elongating conjugate bridges elevate HOMO about 0.13 eV, decline LUMO about 0.13 eV, and reduced E_g. Introducing –CH=CH_2 to TPA moieties generates a similar effect for HOMO, LUMO, and E_g. Also, the calculated E_g reproduced the relative positions of experimental E_g, which were obtained in terms of electrochemical data about redox properties [20]. For instance, the calculated E_g of TPAR1 (2.98 eV) is about 0.07 eV larger than that of TPAR4 (2.91 eV). This agrees well with that of electrochemical experimental data 0.07 eV [20]. The HOMO level corresponds to the oxidation potential of dye sensitizer [13], and the larger

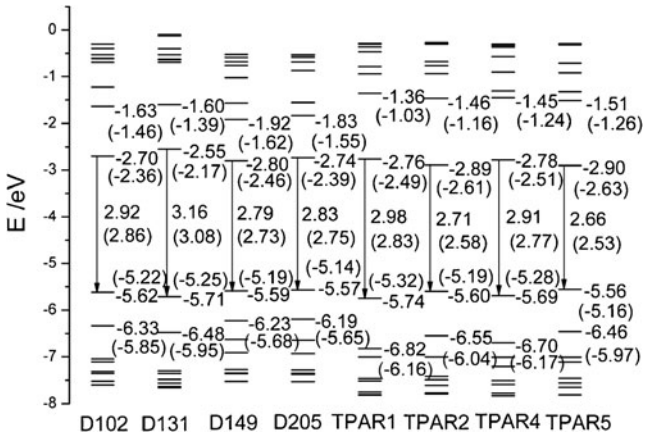

Fig. 2 The calculated frontier molecular orbitals energies and HOMO-LUMO gap at the PBE0/6–31+G(d,p) level in solvent. The corresponding data in parentheses were calculated at the B3LYP/6–31G* in vacuum

oxidation potential increases the reduction driving force of oxidized dye [72]. The reduction driving forces of the oxidized D131 and TPAR1 dyes are slightly larger than that of other dyes because of their lower HOMO level.

Dipole moments and polarizabilities

Once dye molecule adsorbs on the surface of TiO_2, it induces a dipole field, which can shift the conduction band of TiO_2, and thereby affect open-circuit voltage (V_{oc}) [73]. Also, it has been reported that hemicyanine dye sensitizer, which has a prominent nonlinear optical property, usually possesses good photoelectric conversion efficiency [74]. Our previous theoretical studies of several organic dye sensitizers indicated that the dyes with larger isotropic polarizability α usually correspond to a larger extent of electron delocalization and insufficient charge separation in excited CT states [68]. The dipole moments and polarizabilities of the indoline and TPA dyes were calculated in order to understand the effects of performance in DSC. The following formula was adopted to calculate the dipole moment μ,

$$\mu = \sqrt{\mu_x^2 + \mu_y^2 + \mu_z^2}, \quad (1)$$

where μ_x, μ_y, μ_z are vector components of dipole moment. The definitions of the isotropic polarizability α were presented by Christiansen *et al.* [75],

$$\alpha = \frac{1}{3}(\alpha_{XX} + \alpha_{YY} + \alpha_{ZZ}), \quad (2)$$

where α_{xx}, α_{yy}, α_{zz} are tensor components of polarizability. The results are listed in Table 4. The substitution of indoline dyes significantly affect dipole moments due to the substitution change the positive and negative charge-center distance, and also affect the charge-center positions. For TPA-based dyes, the longer conjugate bridges also extend the positive and negative charge-center distance, and thus generate a larger dipole moment. Furthermore, we can find a general tendency that the larger dye molecules usually possess larger polarizabilities. This results from the observation

Table 4 The dipole moment and polarizabilities of the dyes

Dyes	Dipole moment(a.u.)	Polarizabilities(a.u.)
D102	3.60	589
D131	2.91	482
D149	2.67	722
D205	3.82	794
TPAR1	3.44	406
TPAR2	3.70	488
TPAR4	3.37	450
TPAR5	3.65	533

Table 5 The electronic absorption λ_{max} of the dyes

Dyes	Theoretical λ_{max} (nm)					Exp. λ_{max} (nm)
	Gas phase	Solvent				
	B3LYP/6–31G (d)	B3LYP/6–31G (d)	PBE0/6–31G(d, p)	PBE0/6–31+G(d, p)	CAM-B3LYP/6–31+G(d, p)	
D102	474	528	501	503	425	494 [40] 491 [48]
D131	423	480	459	466	401	425 [48]
D149	505	571	536	535	444	526 [40] 526 [48]
D205	501	552	526	527	442	532 [40]
TPAR1	471	520	498	498	434	458 [20]
TPAR2	512	570	543	546	466	476 [20]
TPAR4	487	538	513	512	438	461 [20]
TPAR5	528	586	556	559	469	474 [20]

that the larger dye molecules with conjugate groups enhance electron delocalization, which is favorable for electron transfer from the donor to acceptor in the dye molecules.

Absorption properties

The electronic absorption λ_{max} values of experimental and different theoretical methods are listed in Table 5. It can be found that, the PBE0 results of indoline dyes agree well with the experiment, but for TPA dyes, the CAM-B3LYP/6–31+G(d,p) results agree well with that of the experimental data, especially for the dyes with longer conjugate bridges. So the PBE0 and CAM-B3LYP results are adopted for analyzing the spectral features of indoline and TPA dyes, respectively.

To obtain the microscopic information about the electronic transitions, we check the corresponding MO properties. The absorption in visible and near-UV region is the most important region for photo-to-current conversion, so only the singlet→singlet transitions of the absorption bands with the wavelength longer than 300 nm and the oscillator strength larger than 0.1 are listed in Tables 6 and 7. The isodensity plots of the frontier MOs that relate to the absorption in visible and near-UV region are presented in Fig. 3. The HOMOs of these dyes are quite delocalized from the donor and conjugate bridge parts, whereas the LUMOs of the dyes are mainly located on the acceptor and conjugate bridge groups. The maximum absorptions in UV/vis spectra approximately arise from HOMO→LUMO single configuration π→π* transitions. Furthermore, the main overlap between HOMO and LUMO of the dyes suggest the maximum absorptions have some local

Table 6 The calculated excitation energies (eV), wavelength (nm), electronic transition configurations, oscillator strengths (f) and the short circuit photocurrent density J_{sc}(mA.cm^{-2}) for the singlet→singlet transitions of the absorption band in visible and ultraviolet region for the indoline dyes in THF (PBE0/6–31+G(d,p))

Dyes	Excited states	Assignment (only the configurations composition larger than 10 % were listed)	E(eV/nm)	*f*	J_{sc}[a]
D102	1	H→L (97 %)	503/2.46	1.3366	5.5
	3	H-1→L (91 %)	387/3.20	0.3469	
	4	H→L+1(90 %)	366/3.39	0.3695	
D131	1	H→L (97 %)	466/2.66	1.0905	9.0
	2	H-1→L (55 %); H→L+1(41 %)	363/3.42	0.4639	
	3	H→L+1(55 %); H-1→L (43 %)	349/3.56	0.2125	
D149	1	H→L (95 %)	535/2.32	1.3749	11.08
	2	H-1→L (89 %)	417/2.97	0.3651	
	4	H→L+1(86 %)	392/3.16	0.4402	
	5	H-2→L (74 %); H→L+2(19 %)	369/3.36	0.1737	
	6	H→L+2(72 %); H-2→L (16 %)	351/3.53	0.2066	
D205	1	H→L (96 %)	527/2.35	1.4946	18.99
	2	H-1→L (93 %)	412/3.01	0.3293	
	4	H→L+1(86 %)	385/3.22	0.4710	
	6	H→L+2(56 %); H-2→L (32 %)	348/3.57	0.2141	

[a]The references of experimental J_{sc} are the same as those in the text

Table 7 The calculated excitation energies (eV), wavelength (nm), electronic transition configurations, oscillator strengths (f) and the short circuit photocurrent density J_{sc}(mA.cm^{-2}) for the singlet→singlet transitions of the absorption band in visible and ultraviolet region for the TPA dyes in THF (CAM-B3LYP/6-31+G(d,p))

Dyes	Excited states	Assignment (only the configurations composition larger than 10 % were listed)	E(eV/nm)	*f*	J_{sc}[a]
TPAR1	1	H→L (88 %)	434/2.86	1.3631	13.0
TPAR2	1	H→L (86 %)	466/2.66	1.7406	2.2
	3	H-1→L (75 %); H→L+1(10 %)	329/3.77	0.1175	
TPAR4	1	H→L (85 %)	438/2.83	1.3911	18.2
	3	H-1→L (54 %); H→L+1(24 %)	316/3.93	0.2511	
	4	H→L+2(44 %); H→L+1(18 %) H-1→L (12 %)	305/4.07	0.2112	
TPAR5	1	H→L (83 %)	469/2.64	1.7490	4.5
	3	H-1→L (68 %); H→L+1(13 %)	335/3.70	0.2501	
	4	H→L+2(58 %); H→L+1(13 %)	312/3.98	0.3062	

[a] The references of experimental J_{sc} are the same as those in the text

excited transitions in the conjugate bridge. However, the relocations from the HOMOs to LUMOs indicate that the transitions at maximum absorptions have IMCT character. So the transitions near λ_{max} are not pure CT excitations, which can form complete charge separated states. The further MO analysis indicates that the TPA and 4-(2,2 diphenylethenyl)-phenyl substituent indoline groups are effective chromophores in IMCT. So, these groups play important roles in the sensitization of DSC. The MOs of D205 suggest that the octyl chain has no contributions to the MOs related to IMCT, and

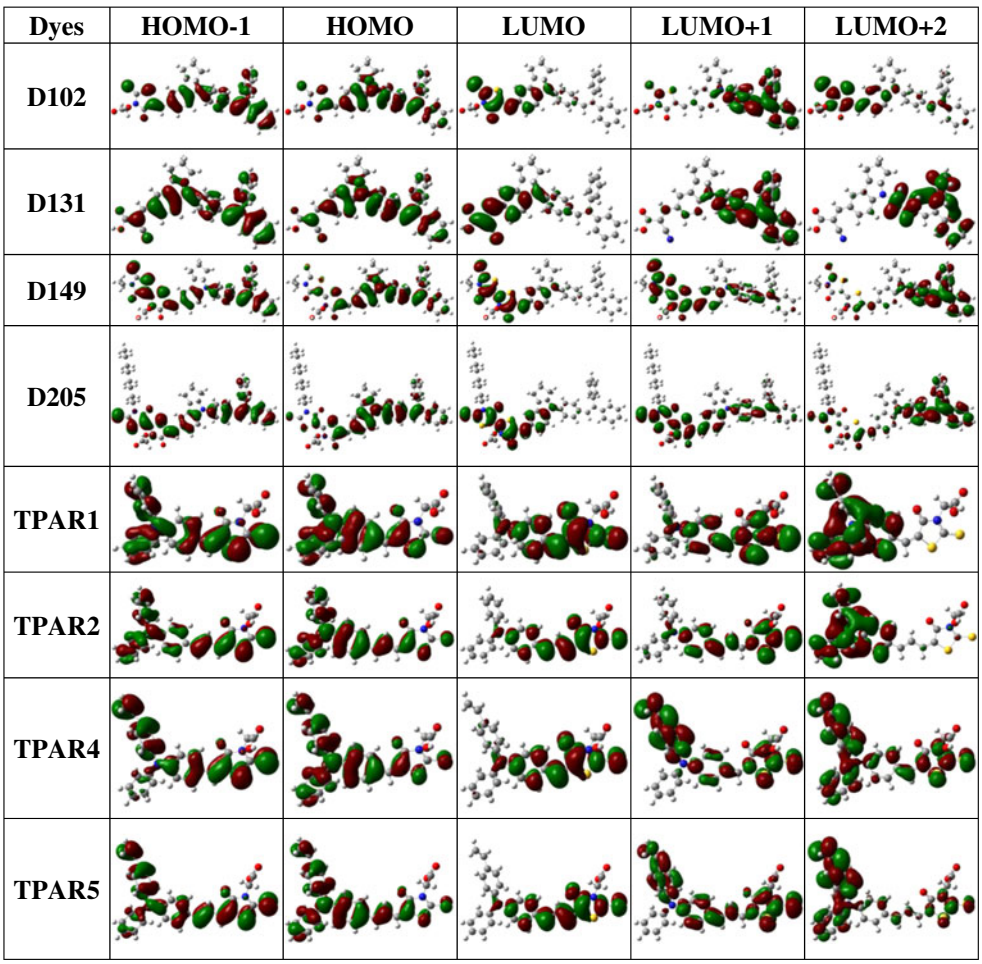

Fig. 3 Isodensity plots (isodensity contour = 0.02 a.u.) of the frontier orbitals of the indoline and TPA-based dyes

thus it does not contribute to enhancing the light harvesting. However, it affects electronic structure, including HOMO and LUMO, and then affects the kinetics of electron injection and dye regeneration. The short-circuit photocurrent density (J_{sc}) of D205 is larger than that of other indoline dyes. This results from the D205 has more IMCT excited states with larger oscillator strength. The larger oscillator strength generates shorter lifetime of excited CT states, and thus a fast CT process, then larger J_{sc}.

Light harvesting efficiencies, the driving force of electron injection and dye regeneration

The light harvesting efficiencies (LHE) of the dye should be as high as possible to increase the photocurrent if the excited processes have CT character. LHE can be calculated as [55]:

$$\mathrm{LHE} = 1 - 10^{-\mathrm{A}} = 1 - 10^{-\mathrm{f}}, \tag{3}$$

where A is absorption coefficient and f is oscillator strength of the dye associated to the $\lambda_{\max}^{(1)}$. Though TDDFT is less efficient for the evaluation of transition probabilities than for transition energies [55], the relative strength for different absorption bands of the dyes were qualitatively reproduced. For instance, the experimental molar absorption coefficients for D149 at $\lambda_{\max}^{(1)}$ and $\lambda_{\max}^{(2)}$ are about 68,000 and 32,000 $\mathrm{M^{-1}cm^{-1}}$ [45], respectively. The calculated oscillator strength at $\lambda_{\max}^{(1)}$ and $\lambda_{\max}^{(2)}$ are 1.3749 and 0.4402 (PBE0), respectively. Taking into account UV–Vis width at half-height to simulate the spectra, the agreement with experiment of relative strength will be better. Furthermore, it had been reported that the dependence of the experimental extinction coefficient with respect to auxochromic effects was qualitatively reproduced for the TPA derivatives [76]. So, the TDDFT results for dyes in this work are reliable for describing relative LHE. For indoline dyes, both the PBE0 and CAM-B3LYP results in Table 8 suggest that D205 has the largest LHE. Whereas for TPA dyes, the longer conjugate bridges of TPAR2 and TPAR5 enhance the overlap of ground states (mainly contributed by HOMO) and the first excited states (mainly contributed by LUMO), and then generate the larger oscillator strength and LHE. Comparing the LHE of D102 and TPAR1 indicates that the LHE of indoline-based dye is higher than that of the corresponding TPA-based dye. This means that the indoline dye has more efficient light harvesting capability than TPA-based dye.

The electron injection from the excited dyes to the semiconductor conduction band and the dye regeneration processes can be described as CT reaction. In terms of Marcus theory for electron transfer [77], the CT rate constants can be affected by the free energy change related to the reaction. The free energy change for electron injection (ΔG^{inject}) affects the electron injection rate and therefore the J_{sc} in DSCs. ΔG^{inject} can be viewed as the electron injection driving force [78]. According to Preat's method [55], assuming the electron injection occurs from the unrelaxed excited state of the dye, the ΔG^{inject} can be calculated by the following equations,

$$\Delta G^{inject} = E_{OX}^{dye*} - E_{CB}^{SC}, \tag{4}$$

where E_{OX}^{dye*} is the oxidation potential of the dye in the excited state and E_{CB}^{SC} is the reduction potential of the conduction band of the semiconductor. The reported E_{CB}^{SC} =4.0 eV for TiO_2 [79] was adopted in this work. The E_{OX}^{dye*} can be calculated as follows [80]:

$$E_{OX}^{dye*} = E_{OX}^{dye} - \lambda_{\max}, \tag{5}$$

where E_{OX}^{dye} is the redox potential of the ground state and $\lambda_{\max}$ is the absorption maximum with IMCT character. Whereas the free energy change of dye regeneration (ΔG_{dye}^{regen}) can affect the rate constant of redox process between the oxidized dyes and electrolyte. The ΔG_{dye}^{regen} can be calculated as:

$$\Delta G_{dye}^{regen} = E_{redox}^{electrolyte} - E_{OX}^{dye}, \tag{6}$$

where $E_{redox}^{electrolyte}$ is the redox potential of electrolyte. The $E_{redox}^{electrolyte}$ of commonly used redox couple iodide/triiodide is

Table 8 The calculated light harvesting efficiencies (LHE), the free energy change for the electron injection (ΔG^{inject}, in eV), the oxidation potential of the dye in excited state (E_{OX}^{dye}, in eV), the oxidation potential of the dye in ground state (E_{OX}^{dye*}, in eV), and the free energy change for the dye regeneration (ΔG^{regen}, in eV)

Dye	LHE	ΔG^{inject}	ΔG^{regen}	E_{OX}^{dye}	E_{OX}^{dye*}
PBE0					
D102	0.9539	−0.84	0.77	5.62	3.16
D131	0.9188	−0.95	0.86	5.71	3.05
D149	0.9578	−0.73	0.74	5.59	3.27
D205	0.9680	−0.78	0.72	5.57	3.22
TPAR1	0.9288	−0.75	0.89	5.74	3.25
TPAR2	0.9620	−0.67	0.75	5.60	3.33
TPAR4	0.9249	−0.63	0.84	5.69	3.27
TPAR5	0.9564	−0.66	0.71	5.56	3.34
CAM-B3LYP					
D102	0.9839	−0.34	1.73	6.58	3.66
D131	0.9658	−0.41	1.83	6.68	3.59
D149	0.9884	−0.24	1.71	6.56	3.76
D205	0.9896	−0.27	1.68	6.53	3.73
TPAR1	0.9567	−0.15	1.86	6.71	3.85
TPAR2	0.9818	−0.11	1.70	6.55	3.89
TPAR4	0.9594	−0.18	1.79	6.64	3.82
TPAR5	0.9822	−0.14	1.65	6.50	3.86

about −4.85 eV (0.35 V vs. NHE) [81]. The calculated E_{OX}^{dye}, E_{OX}^{dye*}, ΔG^{inject}, and ΔG_{dye}^{regen} for all the dyes with PBE0 and CAM-B3LYP functionals are listed in Table 8.

The calculated results indicate that the ΔG^{inject} of the dyes are negative, which means that the dye excited state with IMCT character lies above the TiO_2 conduction band edge. For indoline dyes, the ΔG^{inject} of D131 is larger than that of other dyes, and the ΔG^{inject} of D102, D205, D149 increases in the order. This suggests that introducing a strong electron withdrawing moiety in the acceptor increase the ΔG^{inject}, and then decrease the driving force of electron injection. For TPA dyes, elongating bridge and introducing $–CH_2$ in the donor increase the ΔG^{inject}, and then reduce the driving force of electron injection. The ΔG_{dye}^{regen} of D131 is larger than that of other indoline dyes, and the ΔG_{dye}^{regen} of D102, D149, and D205 are quite similar. The smallest ΔG_{dye}^{regen} of D205 is confirmed by the measurement of electron lifetimes, which showed that the indoline dye sensitizer D205 was highly effective in suppressing electron recombination [40]. This suggests that the D131 has the largest rate constant for regeneration. For TPA dyes, the larger ΔG_{dye}^{regen} of TPAR1 and TPAR4 indicate elongating bridge and introducing $–CH_2$ in the donor decreases the ΔG_{dye}^{regen}. The smaller ΔG_{dye}^{regen} is not favorable for the regeneration of the excited dyes. Also, comparing the ΔG^{inject} and ΔG_{dye}^{regen} of D103 and TPAR1 suggests that the electron injection rate of indoline dye might be faster than that of the corresponding TPA-based dye, while the dye regeneration rate of indoline dye might be slower than that of TPA-based dye.

Conclusions

The computations of the geometries, electronic structures, dipole moments and polarizabilities for TPA-based dyes and indoline dye sensitizers, including TPAR1, D102, D131, D149, D205, TPAR2, TPAR4, and TPAR5, were performed using DFT, and the electronic absorption properties were investigated *via* TD-DFT with PCM for solvent effects. Based upon the theoretical calculations and the reported experimental results of dye sensitizers and DSC, we find the following:

(1) The population analysis suggests that the charges of similar acceptors in different dyes are very similar, but the charges of donors and conjugate bridges are more flexible. The populations also indicate that the donating electron capability of TPA is better than that of indoline.
(2) Introducing another rhodanine-based moiety to indoline dyes with rhodanine-3-acetic acid induces a slight upshift for HOMO and down-shift for LUMO energies. Introducing $–CH=CH_2$ to TPA moieties and conjugate bridges elevate HOMO, decline LUMO, and reduced E_g. The reduction driving force for the oxidized D131 and TPAR1 may be slightly larger than that of other dyes because of their lower HOMO level.
(3) The absorption properties and MO analysis indicate that the TPA and 4-(2,2 diphenylethenyl)phenyl substituent indoline groups are effective chromophores in IMCT, and they play an important role in sensitization of DSCs.
(4) The better performance of indoline and TPA dyes in DSCs are ascribed to different reasons. The larger short-circuit photocurrent density (J_{sc}) of D205 results from more IMCT excited states with larger oscillator strength, the higher LHE of D205 is also helpful for improving the performance in DSCs. While for TPA dyes, the longer conjugate bridges of TPAR2 and TPAR5 enhance the overlap of ground states and the first excited states, and then generate the larger oscillator strength and LHE.
(5) For indoline dyes, D131 has the largest ΔG^{inject} and ΔG_{dye}^{regen}, which are favorable for fast CT, while for TPA dyes, elongating conjugate bridge reduces the ΔG^{inject} and ΔG_{dye}^{regen}. The data of LHE, ΔG^{inject} and ΔG_{dye}^{regen} suggest that the indoline dye has more efficient light harvesting capability, faster electron injection rate, and slower dye regeneration rate than TPA-based dyes.

Acknowledgments This work supported by the Basic Scientific Research Foundation for Gansu Universities of China (Grant No. 1210ZTC055), National Natural Science Foundation of China (Grant Nos. 11164016, 11164015), and scientific developmental foundation of Lanzhou University of Technology. The authors gratefully wish to appreciate the reviewers for reviewing the manuscript and making important suggestions.

References

1. Oregan B, Gratzel M (1991) Nature 353:737–740
2. Gratzel M (2001) Nature 414:338–344
3. Gratzel M (2003) J Photochem Photobio C 4:145–153
4. Nazeeruddin MK, Klein C, Liska P, Gratzel M (2005) Coord Chem Rev 249:1460–1467
5. Li B, Wang L, Kang B, Wang P, Qiu Y (2006) Sol Energy Mater Sol Cells 90:549–573
6. Gratzel M (2009) Acc Chem Res 42:1788–1798
7. Mishra A, Fischer MKR, Bauerle P (2009) Angew Chem Int Ed 48:2474–2499
8. Ning ZJ, Tian H (2009) Chem Commun :5483–5495
9. Robertson N (2006) Angew Chem Int Ed 45:2338–2345
10. Zakeeruddin SM, Gratzel M (2009) Adv Funct Mater 19:2187–2202
11. Clifford JN, Martinez-Ferrero E, Viterisi A, Palomares E (2011) Chem Soc Rev 40:1635–1646

12. Gratzel M (2005) Inorg Chem 44:6841–6851
13. Nazeeruddin MK, Kay A, Rodicio I, Humphrybaker R, Muller E, Liska P, Vlachopoulos N, Gratzel M (1993) J Am Chem Soc 115:6382–6390
14. Nazeeruddin MK, Pechy P, Renouard T, Zakeeruddin SM, Humphry-Baker R, Comte P, Liska P, Cevey L, Costa E, Shklover V, Spiccia L, Deacon GB, Bignozzi CA, Gratzel M (2001) J Am Chem Soc 123:1613–1624
15. Chen XY, Guo JH, Peng XJ, Guo M, Xu YQ, Shi L, Liang CL, Wang L, Gao YL, Sun SG, Cai SM (2005) J Photochem Photobio A 171:231–236
16. Sayama K, Tsukagoshi S, Mori T, Hara K, Ohga Y, Shinpou A, Abe Y, Suga S, Arakawa H (2003) Sol Energy Mater Sol Cells 80:47–71
17. Wu WJ, Hua JL, Jin YH, Zhan WH, Tian H (2008) Photochem Photobio Sci 7:63–68
18. Chen YS, Li C, Zeng ZH, Wang WB, Wang XS, Zhang BW (2005) J Mater Chem 15:1654–1661
19. Wang ZS, Li FY, Huang CH (2001) J Phys Chem B 105:9210–9217
20. Liang M, Xu W, Cai FS, Chen PQ, Peng B, Chen J, Li ZM (2007) J Phys Chem C 111:4465–4472
21. Shen P, Tang YH, Jiang SH, Chen HJ, Zheng XY, Wang XY, Zhao B, Tan ST (2011) Org Electron 12:125–135
22. Cappel UB, Karlsson MH, Pschirer NG, Eickemeyer F, Schoneboom J, Erk P, Boschloo G, Hagfeldt A (2009) J Phys Chem C 113:14595–14597
23. Jiao CJ, Zu NN, Huang KW, Wang P, Wu JS (2011) Org Lett 13:3652–3655
24. Li C, Schoneboom J, Liu ZH, Pschirer NG, Erk P, Herrmann A, Mullen K (2009) Chem Eur J 15:878–884
25. Li C, Yum JH, Moon SJ, Herrmann A, Eickemeyer F, Pschirer NG, Erk P, Schoeboom J, Mullen K, Gratzel M, Nazeeruddin MK (2008) Chemsuschem 1:615–618
26. Tian H, Liu PH, Zhu WH, Gao EQ, Da-Jun WA, Cai SM (2000) J Mater Chem 10:2708–2715
27. Hara K, Sato T, Katoh R, Furube A, Ohga Y, Shinpo A, Suga S, Sayama K, Sugihara H, Arakawa H (2003) J Phys Chem B 107:597–606
28. Koops SE, Barnes PRF, O'Regan BC, Durrant JR (2010) J Phys Chem C 114:8054–8061
29. Li XG, Lu HJ, Wang SR, Guo JJ, Li J (2011) Prog Chem 23:569–588
30. Campbell WM, Burrell AK, Officer DL, Jolley KW (2004) Coord Chem Rev 248:1363–1379
31. Hsieh CP, Lu HP, Chiu CL, Lee CW, Chuang SH, Mai CL, Yen WN, Hsu SJ, Diau EWG, Yeh CY (2010) J Mater Chem 20:1127–1134
32. Imahori H, Umeyama T, Ito S (2009) Acc Chem Res 42:1809–1818
33. Lee CW, Lu HP, Lan CM, Huang YL, Liang YR, Yen WN, Liu YC, Lin YS, Diau EWG, Yeh CY (2009) Chem Eur J 15:1403–1412
34. Pasunooti KK, Song JL, Chai H, Amaladass P, Deng WQ, Liu XW (2011) J Photochem Photobio A 218:219–225
35. Wu SL, Lu HP, Yu HT, Chuang SH, Chiu CL, Lee CW, Diau EWG, Yeh CY (2010) Energy Environ Sci 3:949–955
36. Geiger T, Kuster S, Yum JH, Moon SJ, Nazeeruddin MK, Gratzel M, Nuesch F (2009) Adv Funct Mater 19:2720–2727
37. Paek S, Choi H, Kim C, Cho N, So S, Song K, Nazeeruddin MK, Ko J (2011) Chem Commun 47:2874–2876
38. Silvestri F, Lopez-Duarte I, Seitz W, Beverina L, Martinez-Diaz MV, Marks TJ, Guldi DM, Pagani GA, Torres T (2009) Chem. Commun : 4500–4502
39. Cheng HM, Hsieh WF (2010) Nanotechnology 21: 485202 485202
40. Kuang D, Uchida S, Humphry-Baker R, Zakeeruddin SM, Gratzel M (2008) Angew Chem Int Ed 47:1923–1927
41. Zhang XH, Li C, Wang WB, Cheng XX, Wang XS, Zhang BW (2007) J Mater Chem 17:642–649
42. Yella A, Lee H-W, Tsao HN, Yi C, Chandiran AK, Nazeeruddin MK, Diau EW-G, Yeh C-Y, Zakeeruddin SM, Grätzel M (2011) Science 334:629–634
43. Horiuchi T, Miura H, Uchida S (2003) Chem Commun: 3036–3037
44. Horiuchi T, Miura H, Sumioka K, Uchida S (2004) J Am Chem Soc 126:12218–12219
45. Dentani T, Kubota Y, Funabiki K, Jin J, Yoshida T, Minoura H, Miura H, Matsui M (2009) New J Chem 33:93–101
46. Tanaka H, Takeichi A, Higuchi K, Motohiro T, Takata M, Hirota N, Nakajima J, Toyoda T (2009) Sol Energy Mater Sol Cells 93:1143–1148
47. Ito S, Zakeeruddin SM, Humphry-Baker R, Liska P, Charvet R, Comte P, Nazeeruddin MK, Pechy P, Takata M, Miura H, Uchida S, Gratzel M (2006) Adv Mater 18:1202–1205
48. Howie WH, Claeyssens F, Miura H, Peter LM (2008) J Am Chem Soc 130:1367–1375
49. Snaith HJ, Petrozza A, Ito S, Miura H, Gratzel M (2009) Adv Funct Mater 19:1810–1818
50. Zhang Z, Chen P, Murakami TN, Zakeeruddin SM, Gratzel M (2008) Adv Funct Mater 18:341–346
51. Ito S, Miura H, Uchida S, Takata M, Sumioka K, Liska P, Comte P, Pechy P, Gratzel M (2008) Chem Commun: 5194–5196
52. Jose R, Kumar A, Thavasi V, Fujihara K, Uchida S, Ramakrishna S (2008) Appl Phys Lett 93: 023125 023125
53. Le Bahers T, Pauporte T, Scalmani G, Adamo C, Ciofini I (2009) Phys Chem Chem Phys 11:11276–11284
54. Ning ZJ, Zhang Q, Wu WJ, Pei HC, Liu B, Tian H (2008) J Org Chem 73:3791–3797
55. Preat J, Michaux C, Jacquemin D, Perpete EA (2009) J Phys Chem C 113:16821–16833
56. Xu W, Peng B, Chen J, Liang M, Cai F (2008) J Phys Chem C 112:874–880
57. Frisch MJ, Trucks GW, Schlegel HB, Scuseria GE, Robb MA, Cheeseman JR, Scalmani G, Barone V, Mennucci B, Petersson GA, Nakatsuji H, Caricato M, Li X, Hratchian HP, Lzmaylov AF, Bloino J, Zheng G, Sonnenberg JL, Hada M, Ehara M, Toyota K, Fukuda R, Hasegawa J, Ishida M, Nakajima T, Honda Y, Kitao O, Nakai H, Vreven T Jr, Peralta JE, Ogliaro F, Bearpark M, Heyd JJ, Brothers E, Kudin KN, Staroverov VN, Keith T, Kobayashi R, Normand J, Raghavachari K, Rendell A, Burant JC, Lyengar SS, Tomasi J, Cossi M, Rega N, Millam JM, Klene M, Knox JE, Cross JB, Bakken V, Adamo C, Jaramillo J, Gomperts R, Stratmann RE, Yazyev O, Austin AJ, Cammi R, Pomelli C, Ochterski JW, Martin RL, Morokuma K, Zakrzewski VG, Voth GA, Salvador P, Dannenberg JJ, Dapprich S, Daniels AD, Farkas O, Foresman JB, Ortiz JV, Cioslowski J, Fox DJ (2010) Gaussian 09. Gaussian Inc, Wallingford, CT
58. Adamson RD, Dombroski JP, Gill PMW (1999) J Comput Chem 20:921–927
59. Becke AD (1988) Phys Rev A 38:3098–3100
60. Becke AD (1993) J Chem Phys 98:5648–5652
61. Lee CT, Yang WT, Parr RG (1988) Phys Rev B 37:785–789
62. Adamo C, Barone V (1999) J Chem Phys 110:6158–6170
63. Yanai T, Tew DP, Handy NC (2004) Chem Phys Lett 393:51–57
64. Cossi M, Barone V (2000) J Phys Chem A 104:10614–10622
65. Xu J, Wang L, Liang G, Bai Z, Wang L, Xu W, Shen X (2011) Spectrochim Acta Part A 78:287–293
66. Xu J, Zhang H, Wang L, Liang G, Wang L, Shen X, Xu W (2010) Chem Monthly 141:549–555
67. Xu J, Zhu L, Wang L, Liu L, Bai Z, Wang L, Xu W (2012) J Mol Model 18:1767–1777

68. Zhang CR, Liu ZJ, Chen YH, Chen HS, Wu YZ, Yuan LH (2009) J Mol Struct(Theochem) 899:86–93
69. Zhang CR, Liu ZJ, Chen YH, Chen HS, Wu YZ, Feng WJ, Wang DB (2010) Curr Appl Phys 10:77–83
70. Zhang CR, Chen HS, Chen YH, Wei ZQ, Pu ZS (2008) Acta Phys Chim Sin 24:1353–1358
71. Preat J, Michaux C, Jacquemin D, Perpète EA (2009) J Phys Chem C 113:16821–16833
72. Zhang X, Zhang JJ, Xia YY (2008) J Photochem Photobio A 194:167–172
73. De Angelis F, Fantacci S, Selloni A, Grätzel M, Nazeeruddin MK (2007) Nano Lett 7:3189–3195
74. Wang ZS, Huang YY, Huang CH, Zheng J, Cheng HM, Tian SJ (2000) Synth Met 114:201–207
75. Christiansen O, Gauss J, Stanton JF (1999) Chem Phys Lett 305:147–155
76. Preat J, Jacquemin D, Wathelet V, André J-M, Perpète EA (2007) Chem Phys 335:177–186
77. Marcus RA (1993) Rev Mod Phys 65:599–610
78. Fan W, Tan D, Deng W-Q (2012) Chem Phys Chem 13:2051–2060
79. Asbury JB, Wang Y-Q, Hao E, Ghosh HN, Lian T (2001) Res Chem Intermed 27:393–406
80. Katoh R, Furube A, Yoshihara T, Hara K, Fujihashi G, Takano S, Murata S, Arakawa H, Tachiya M (2004) J Phys Chem B 108:4818–4822
81. Boschloo G, Hagfeldt A (2009) Acc Chem Res 42:1819–1826